Ann Neurol. Author manuscript; available in PMC 2016 May 25.

Published in final edited form as:
Ann Neurol. 2015 March ; 77(3): 541–546. doi:10.1002/ana.24342.

Interneuron Activity Leads to Initiation of Low-Voltage Fast-Onset Seizures

Zahra Shiri, BSc[1], **Frédéric Manseau, PhD**[2], **Maxime Lévesque, PhD**[1], **Sylvain Williams, PhD**[2], and **Massimo Avoli, MD, PhD**[1]

[1]Montreal Neurological Institute and Departments of Neurology and Neurosurgery, McGill University Montreal, Quebec, Canada

[2]Douglas Mental Health University Institute, McGill University, Montreal, Quebec, Canada

Abstract

Seizures in temporal lobe epilepsy can be classified as hypersynchronous and low-voltage fast according to their onset patterns. Experimental evidence suggests that low-voltage fast-onset seizures mainly result from the synchronous activity of γ-aminobutyric acid–releasing cells. In this study, we tested this hypothesis using the optogenetic control of parvalbumin-positive interneurons in the entorhinal cortex, in the *in vitro* 4-aminopyridine model. We found that both spontaneous and optogenetically induced seizures had similar low-voltage fast-onset patterns. In addition, both types of seizures presented with higher ripple than fast ripple rates. Our data demonstrate the involvement of interneuronal networks in the initiation of low-voltage fast-onset seizures.

Patients with temporal lobe epilepsy (TLE) present with 2 distinct patterns of seizure onset, which have been termed low-voltage fast (LVF) and hypersynchronous (HYP).[1,2] Similar seizure onset types occur in animal models of TLE.[3,4] LVF seizures usually initiate with 1 or 2 interictal-like (hereafter referred to as “interictal”) spikes followed by low-amplitude, high-frequency activity, whereas HYP onset is characterized by a series of (preictal) focal spikes occurring at approximately 2Hz. LVF and HYP seizures are thought to depend on the activity of distinct neural networks, and it has been shown that LVF ictal-like (hereafter referred to as “ictal”) discharges induced *in vitro* by the K^+ channel blocker 4-aminopyridine (4AP) are (1) initiated by spikes that may reflect the firing of γ-aminobutyric acid (GABA)-releasing cells and (2) sustained by $GABA_A$ receptor signaling.[5] LVF seizures recorded in models of temporal lobe epilepsy are also preferentially linked to ripples (ie, high-frequency oscillations [HFOs] at 80–200Hz)[4,6]; ripples are thought to reflect inhibitory postsynaptic

Address correspondence to Dr Avoli, Montreal Neurological Institute, McGill University, 3801 University Street, Montréal, PQ, Canada, H3A 2B4. massimo.avoli@mcgill.ca.

Authorship

Z.S. performed field recordings, and contributed to data analysis and writing of the manuscript. F.M. performed patchclamp recordings, and contributed to experiment design and writing of the manuscript. M.L. contributed to analysis of the data and writing of the manuscript. S.W. contributed to study design and revising the manuscript. M.A. contributed to study concept and design, and drafting and revising the manuscript for content, including analysis and interpretation of data.

Potential Conflicts of Interest

Nothing to report.

potential (IPSP) populations generated by principal glutamatergic neurons entrained by networks of synchronously active interneurons.[7,8] Moreover, modeling studies have suggested that LVF seizures are linked to the abnormal and continuous generation of IPSPs by inhibitory interneurons that impinge on principal cells.[9] We have therefore tested here the hypothesis that activation of GABA-releasing parvalbumin-positive (PV) interneurons[10] can initiate LVF seizures similar to those occurring spontaneously by employing the optogenetic control of PV interneurons of the entorhinal cortex (EC) in the *in vitro* 4AP model.

Materials and Methods

Animals

We used 21 slices from 14 mice (30–39 days old) expressing channelrhodopsin-2 (ChR2) in parvalbumin-expressing neurons. These animals were generated by breeding PV-Cre and R26-hChR2-EYFP homozygous mice (Jackson Laboratory, Bar Harbor, ME; 008069 and 012569). Mice were deeply anesthetized with inhaled isoflurane and decapitated. Brains were quickly removed and immersed in ice-cold slicing solution containing (in millimolars): 252 sucrose, 10 glucose, 26 $NaHCO_3$, 2 KCl, 1.25 KH_2PO_4, 10 $MgCl_2$, and 0.1 $CaCl_2$ (pH 7.3, oxygenated with 95% O_2/5% CO_2). Horizontal sections (400μm) containing the EC were cut using a vibratome (VT1000S; Leica, Wetzlar, Germany) and kept for at least 1 hour prior to experimentation in a slice saver filled with artificial cerebrospinal fluid (ACSF) of the following composition (in millimolars): 125 NaCl, 25 glucose, 26 $NaHCO_3$, 2 KCl, 1.25 NaH_2PO_4, 2 $MgCl_2$, and 1.2 $CaCl_2$. All procedures were performed according to protocols and guidelines approved by the McGill University Animal Care Committee and Canadian Council on Animal Care.

Local Field Potential, Patch Clamp, and Photostimulation

Slices were transferred to a submerged chamber with continuous perfusion of oxygenated ACSF (KCl and $CaCl_2$ adjusted to 4.5 and 2mM, respectively; 30 °C, 10ml/min), and local field potentials (LFPs) were recorded using ACSF-filled microelectrodes (1–2MΩ) positioned in the EC superficial layers. Signals were recorded with a differential alternating current amplifier (A-M Systems, Sequim, WA), filtered online (0.1–500Hz), digitized with a Digidata 1440a (Axon Instruments, Sunnyvale, CA), and sampled at 5kHz using pClamp software (Axon Instruments). In a subset of experiments (n=3), whole-cell patch-clamp recordings were performed on visually identified interneurons in the EC. Patch electrodes (3–6MΩ) were filled with intrapipette solution containing the following (in millimolars): 144 K-gluconate, 3 $MgCl_2$, 10 N-2- hydroxyethylpiperazine-N′-2-ethanesulfonic acid, 0.2 ethyleneglycoltetraacetic acid, 2 Na_2–adenosine triphosphate, and 0.3 guanosine triphosphate, pH7.3 (285–295mOsm). Signals were amplified using a Multiclamp 700B patch-clamp amplifier (Molecular Devices, Sunnyvale, CA), sampled at 20kHz, and filtered at 10kHz. For ChR2 excitation, blue light (473nm, intensity=35mW) was delivered through a custom-made light-emitting diode (LED) system, where the LED (Luxeon Star LEDs, Brantford, Ontario, Canada) was coupled to a 3mm-wide optical fiber (Edmund Optics, Barrington, NJ) placed above the recording region. Light pulses (1- or 2-second duration) were delivered at 0.2Hz for 30 seconds with a 130-second interval between trains. The temperature of the bath was constantly monitored throughout the experiments, and no

change was observed during the stimulation. 4AP (150μM) was bath applied in all experiments, and in some slices (n=5) we simultaneously added the $GABA_A$ receptor antagonist picrotoxin (50μM), and the $GABA_B$ receptor antagonist CGP55845 (4μM) to the superfusing ACSF. All reagents were obtained from Sigma-Aldrich Canada (Oakville, Ontario, Canada).

Analysis of High-Frequency Oscillations

LFPs were first low-pass filtered at 500Hz and then down-sampled to 2,000Hz to prevent aliasing. A multiparametric algorithm was then used to identify oscillations in each frequency range, using routines based on standardized MATLAB signal processing functions (MathWorks, Natick, MA). For each ictal discharge, raw LFP recordings were bandpass filtered in the 80 to 200Hz and in the 250 to 500Hz frequency range using a finite impulse response filter; zero-phase digital filtering was used to avoid phase distortion. A 10-second artifact-free period (50–40 seconds before ictal discharge onset) was selected as a reference for signal normalization. LFPs were thus normalized using their own reference period. To be considered as an HFO candidate, oscillatory events in each frequency band had to show at least 4 consecutive cycles having an amplitude of 4 standard deviations above the mean of the reference period. The time lag between 2 consecutive cycles had to be between 5 and 12.5 milliseconds for ripples and 2 and 4 milliseconds for fast ripples. Furthermore, special care was taken to avoid the detection of false HFOs, which may be caused by the filtering of sharp spikes.[11] Rates of HFOs (ripples, fast ripples) were computed based on 9 spontaneous and 10 evoked ictal discharges and compared using nonparametric Wilcoxon rank sum tests followed by Bonferroni–Holm corrections for multiple comparisons. Statistical tests were performed in MATLAB using the Statistics Toolbox; the level of significance was set to $p<0.05$.

Results

We analyzed a total of 255 ictal events that were recorded from the EC (n=19 slices). Of these events, 138 occurred spontaneously, 77 were triggered by a train of 1-second pulses, and 40 were triggered by a train of 2-second pulses. Stimuli of 1- and 2-second duration were equally successful (48%; data not shown) in triggering ictal events and were thus pooled together for analysis. Representative examples of spontaneous and evoked ictal events are shown in Figure 1A and B, respectively. In control experiments, the interval between spontaneous ictal discharges was 208.26±11.39 seconds on average. We were able to trigger similar events at a shorter interval of 138.63±5.75 seconds under the same conditions with optogenetic stimulation ($p<0.01$). When the onset of an optically induced ictal discharge was expanded, the pattern was typical of an LVF seizure with 1 or 2 interictal spikes leading to the ictal discharge. The same LVF pattern could be observed at the onset of spontaneous ictal discharges.

To ensure that the evoked discharges are dependent on interneuron activation only, we simultaneously bath applied the $GABA_A$ receptor antagonist picrotoxin (50μM) and $GABA_B$ receptor antagonist CGP55845 (4μM). This pharmacological manipulation effectively abolished all spontaneous and light-induced ictal discharges (n=5; see Fig 1C). Under such

GABA receptor-suppressing conditions, spontaneous rhythmic discharges (duration=1–2 seconds) occurred for the entire length of the recording (~20 minutes) and were not driven by the optogenetic stimulation (see Fig 1C, example expanded on right). As reported in previous studies,[5] these presumptive glutamatergic epileptiform events were different from the interictal discharges recorded under 4AP conditions (see Fig 1C, example expanded on left).

Next, we wanted to test whether direct activation of PV interneurons recorded in whole-cell configuration triggers ictal discharges in nearby field recordings. First, we set out to characterize the cells expressing the channelrhodopsin (n=3). Whole-cell current clamp recordings revealed typical firing activity of fast-spiking PV interneurons (Fig 2). Using optogenetic stimulation, we were able to repeatedly activate these interneurons and trigger ictal discharges with an LVF onset pattern. These cells remained viable following optogenetic stimulation, as they consistently responded to stimuli over time.

We also examined the rate and pattern of HFO occurrence throughout the ictal discharges recorded in the EC (Fig 3A). Ripple rates were higher than fast ripple rates throughout both spontaneous and light-triggered ictal discharges as expected for an LVF discharge ($p<0.01$).[4] HFO rates were highest at the onset of the event in both spontaneous and stimulated ictal discharges and gradually decreased throughout the event (see Fig 3B, C).

Discussion

The involvement of interneurons in the initiation of ictal discharges has been suggested based on *in vivo*[12] and *in vitro*[13–15] results. Here, we show that GABA release due to the optogenetic activation of PV interneurons could lead to LVF ictal discharges *in vitro*. First, we discovered that during bath application of 4AP, EC neuronal networks generate ictal discharges that are characterized by an LVF onset pattern and can either occur spontaneously or be triggered by PV interneuron activation. Second, we triggered similar events in the whole-cell configuration by optically activating PV interneurons. Finally, we identified patterns of HFO occurrence that were similar during both types of ictal events and were predominated by ripple rates.

Our group has previously shown that the systemic administration of 4AP *in vivo*[16] and its bath application *in vitro*[17] induces LVF type seizures with similar morphological features. Lévesque et al[16] also reported that *in vivo* 4AP treatment induces sustained and rhythmic runs of theta oscillations that are thought to play a role in ictogenesis. [18] These theta oscillations are presumably caused by GABAergic inputs to pyramidal cells as they are abolished by the $GABA_A$ receptor antagonist, picrotoxin.[19] Other electrophysiological data have revealed a long-lasting GABAergic potential that reflects the synchronous activity of interneurons at the onset of LVF ictal discharges. [5] Therefore, our study demonstrates that GABAergic mechanisms are responsible for LVF seizures, because we could trigger ictal discharges with LVF onset patterns (similar to what is occurring spontaneously) by locally and transiently activating PV-positive EC interneurons.

It has been previously reported that in LVF seizures, the transition from interictal to ictal activity is characterized by higher ripple rates at seizure onset.[4] In line with these results, we found higher ripple rates at the onset of both spontaneous and optogenetically induced ictal discharges during 4AP application. Although the exact mechanisms underlying the generation of ripples is not known, it has been suggested that ripples reflect summated IPSPs generated by principal cells in response to the inhibitory action of interneurons. Therefore, our findings further highlight the involvement of interneuronal networks in initiating LVF-onset seizures, which are then, at least partially, maintained by the persistent firing of principal cells.

Our findings clearly identify the pivotal involvement of GABAergic interneurons in the initiation and maintenance of LVF seizures in the limbic system. Additional studies should investigate whether activating glutamatergic principal cells in the EC leads to HYP onset seizures. Combining these results could help identify more efficacious antiepileptic strategies aimed specifically at targeting GABAergic or glutamatergic neuronal network excitability.

Acknowledgments

This study was supported by the Canadian Institutes of Health Research (grants 8109 and 74609, M.A.; MOP119340, S.W.).

References

1. Ogren JA, Wilson CL, Bragin A, et al. Three-dimensional surface maps link local atrophy and fast ripples in human epileptic hippocampus. Ann Neurol. 2009; 66:783–791. [PubMed: 20035513]
2. Velasco AL, Wilson CL, Babb TL, Engel J Jr. Functional and anatomic correlates of two frequently observed temporal lobe seizure-onset patterns. Neural Plast. 2000; 7:49–63. [PubMed: 10709214]
3. Bragin A, Azizyan A, Almajano J, et al. Analysis of chronic seizure onsets after intrahippocampal kainic acid injection in freely moving rats. Epilepsia. 2005; 46:1592–1598. [PubMed: 16190929]
4. Lévesque M, Salami P, Gotman J, Avoli M. Two seizure-onset types reveal specific patterns of high-frequency oscillations in a model of temporal lobe epilepsy. J Neurosci Off J Soc Neurosci. 2012; 32:13264–13272.
5. Avoli M, de Curtis M. GABAergic synchronization in the limbic system and its role in the generation of epileptiform activity. Prog Neurobiol. 2011; 95:104–132. [PubMed: 21802488]
6. Panuccio G, Sanchez G, Lévesque M, et al. On the ictogenic properties of the piriform cortex *in vitro*. Epilepsia. 2012; 53:459–468. [PubMed: 22372627]
7. Jefferys, JGR., Jiruska, P., de Curtis, M., Avoli, M. Noebels, JL.Avoli, M.Rogawski, MA., et al., editors. [Accessed January 17, 2014] Limbic network synchronization and temporal lobe epilepsy. Jasper's basic mechanisms of the epilepsies. Available at: http://www.ncbi.nlm.nih.gov/books/NBK98158/
8. Aivar P, Valero M, Bellistri E, de la Prida LM. Extracellular calcium controls the expression of two different forms of ripple-like hippocampal oscillations. J Neurosci. 2014; 34:2989–3004. [PubMed: 24553939]
9. Wendling F, Bartolomei F, Bellanger JJ, Chauvel P. Epileptic fast activity can be explained by a model of impaired GABAergic dendritic inhibition. Eur J Neurosci. 2002; 15:1499–1508. [PubMed: 12028360]
10. DeFelipe J, López-Cruz PL, Benavides-Piccione R, et al. New insights into the classification and nomenclature of cortical GABAergic interneurons. Nat Rev Neurosci. 2013; 14:202–216. [PubMed: 23385869]

11. Bénar CG, Chauvière L, Bartolomei F, Wendling F. Pitfalls of high-pass filtering for detecting epileptic oscillations: a technical note on “false” ripples. Clin Neurophysiol Off J Int Fed Clin Neurophysiol. 2010; 121:301–310.
12. Grasse DW, Karunakaran S, Moxon KA. Neuronal synchrony and the transition to spontaneous seizures. Exp Neurol. 2013; 248:72–84. [PubMed: 23707218]
13. Dzhala VI, Staley KJ. Transition from interictal to ictal activity in limbic networks *in vitro*. J Neurosci. 2003; 23:7873–7880. [PubMed: 12944517]
14. Zhang ZJ, Koifman J, Shin DS, et al. Transition to seizure: ictal discharge is preceded by exhausted presynaptic GABA release in the hippocampal CA3 region. J Neurosci Off J Soc Neurosci. 2012; 32:2499–2512.
15. Gnatkovsky V, Librizzi L, Trombin F, de Curtis M. Fast activity at seizure onset is mediated by inhibitory circuits in the entorhinal cortex *in vitro*. Ann Neurol. 2008; 64:674–686. [PubMed: 19107991]
16. Lévesque M, Salami P, Behr C, Avoli M. Temporal lobe epileptiform activity following systemic administration of 4-aminopyridine in rats. Epilepsia. 2013; 54:596–604. [PubMed: 23521339]
17. Avoli M, Panuccio G, Herrington R, et al. Two different interictal spike patterns anticipate ictal activity *in vitro*. Neurobiol Dis. 2013; 52:168–176. [PubMed: 23270790]
18. Butuzova MV, Kitchigina VF. Repeated blockade of GABAA receptors in the medial septal region induces epileptiform activity in the hippocampus. Neurosci Lett. 2008; 434:133–138. [PubMed: 18304731]
19. Buzsáki G. Theta oscillations in the hippocampus. Neuron. 2002; 33:325–340. [PubMed: 11832222]

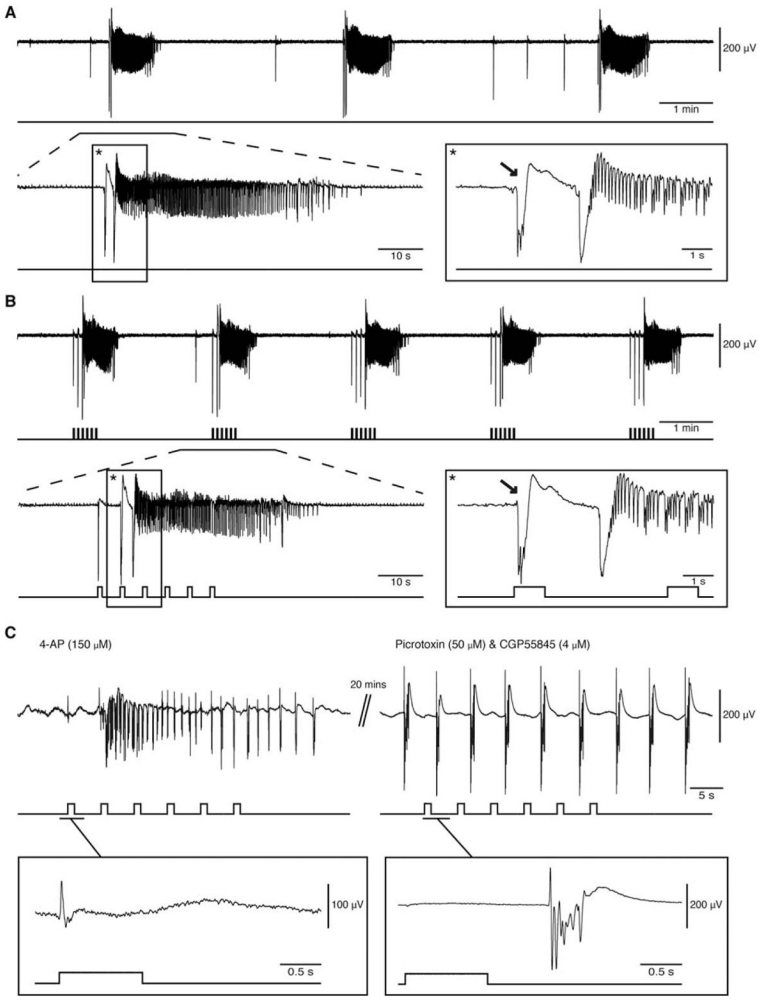

FIGURE 1.

Low-voltage fast ictal discharges can occur spontaneously or be triggered by optogenetic activation of parvalbumin-positive interneurons. (A) Spontaneous ictal discharges occurring during bath application of 4-aminopyridine (4AP); 1 of the events is further expanded to show the onset pattern *(asterisks)*. (B) Ictal discharges evoked by 1-second light pulses during bath application of 4AP; 1 of the events is further expanded to compare the onset patterns *(asterisks)*. Note that in both A and B, the ictal discharge is preceded by a negative-going interictal field potential *(arrows)*. (C) Changes induced by concomitant bath application of picrotoxin and CGP55845 on the ictal discharge evoked by a train of 1-second light pulses (4AP, 150μM panel). Note that under control conditions, the first light pulse induces a positive-going monospike (expanded example) that is followed by ictal synchronization, whereas during γ-aminobutyric acid $(GABA)_A$ and $GABA_B$ receptor antagonism both ictal discharge and the ability of light pulses to drive interictal events are abolished. Under these conditions, negative-going polyspikes (expanded example) occur regardless of the light pulses for at least 20 minutes (maximum time recorded); note the different vertical scales in the expanded examples.

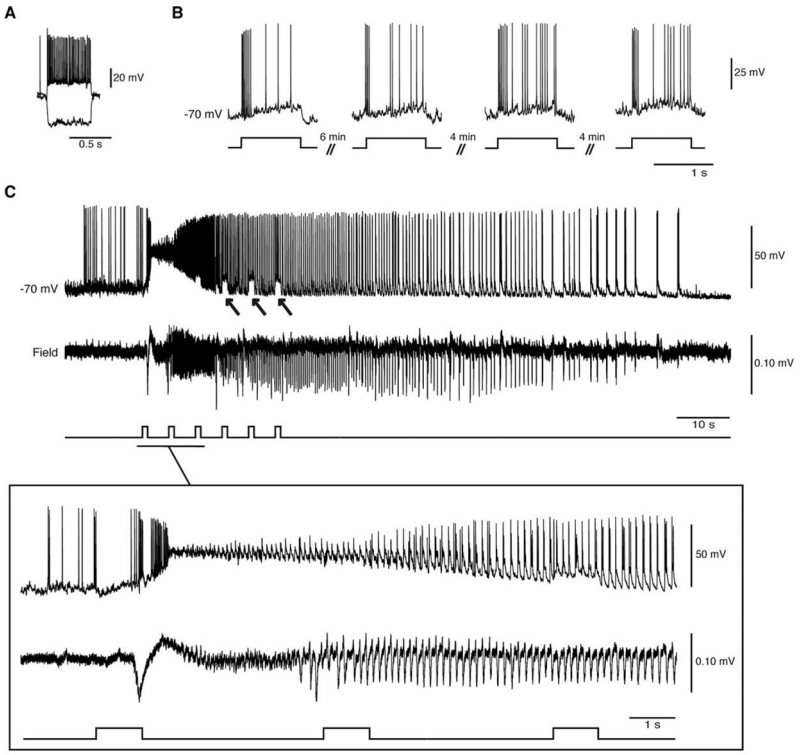

FIGURE 2.

Optogenetic activation of parvalbumin-positive (PV) interneurons in the whole-cell configuration triggers low-voltage fast (LVF) ictal discharges. (A) Electrophysiological characterization of an entorhinal cortex fast-spiking PV interneuron during injection of hyperpolarizing and depolarizing current pulses (V_m=−70mV; intracellular current pulses=600 milliseconds, −200 and 160pA). (B) Responses to 1-second light pulses recorded from the same cell at 4 different time points. Note that similar action potential discharges are generated over time. (C) Optogenetic activation of this interneuron (and of the concomitant LVF ictal discharge) by a train of 1-second light pulses; note the arrows pointing to the pulse-induced depolarizations during the ictal discharge. The onset of the ictal event is expanded below to further reveal the LVF pattern.

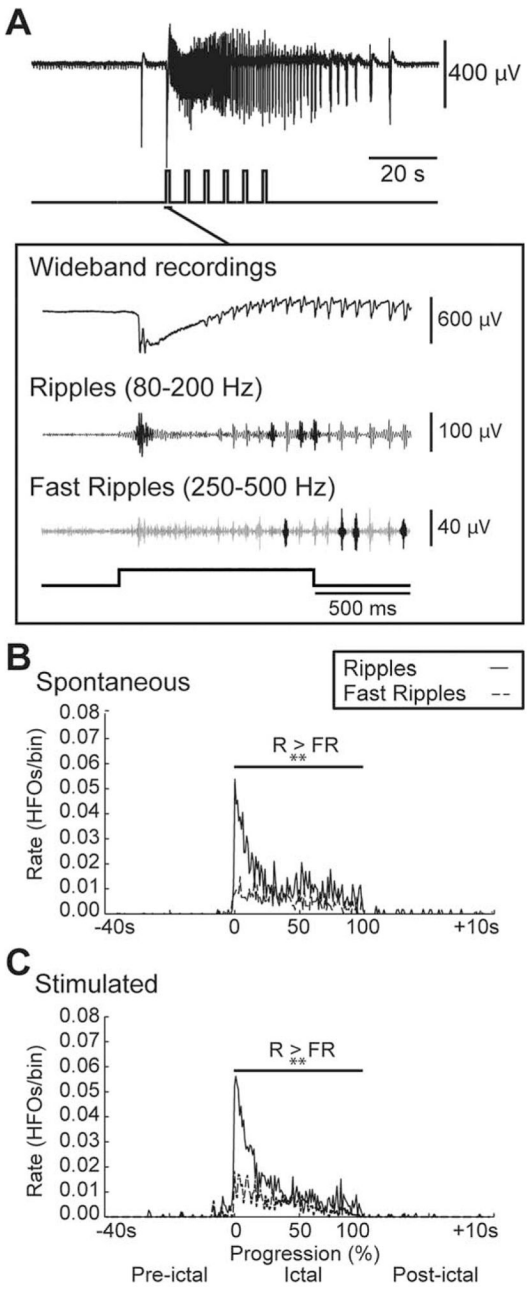

FIGURE 3.

Similar patterns of high-frequency oscillations (HFOs) characterize spontaneous and light-triggered ictal discharges. (A) Ictal discharge stimulated by a train of 1-second light pulses and expanded onset illustrating wide-band recording and filtered traces of associated ripples and fast ripples that are highlighted in darker gray. (B, C) Average rate of ripples (R) and fast ripples (FR) in the 40 seconds preceding, during, and 10 seconds following spontaneous (n=9 events) and stimulated (n=10 events) ictal discharges, respectively. The duration of the ictal discharges was normalized with 0 representing their start and 100 representing their end. Note that ripple rates are higher than fast ripple rates throughout spontaneous and

stimulated ictal discharges as well as that both types of HFO are characterized by highest rates at the onset of the event and gradually decrease throughout the event; $^{**}p < 0.01$.